A study on the phase behavior of poly(ε-caprolactone)-poly(butadiene) diblock copolymers: The influence of relatively low-molecular-weight block copolymers on the order-disorder transition behavior

Hideaki Takagi[a,*], *Katsuhiro Yamamoto*[b,*], *Shigeru Okamoto*[b], *Shinichi Sakurai*[c]

[a]*Photon Factory, Institute of Materials Structure Science, High Energy Accelerator Research Organization, 1-1 Oho, Tsukuba, Ibaraki 305-0801, Japan*

[b]*Department of Materials Science & Engineering, Graduate School of Engineering, Nagoya Institute of Technology, Gokiso-cho, Showa-ku, Nagoya 466-8555, Japan*

[c]*Department of Biobased Materials Science, Graduate School of Science & Technology, Kyoto Institute of Technology, Matsugasaki, Sakyo-ku, Kyoto 606-8585, Japan*

[*] Corresponding authors.

E-mail address: takagih@post.kek.jp (H. Takagi), yamamoto.katsuhiro@nitech.ac.jp (K. Yamamoto)

Graphical Abstract:

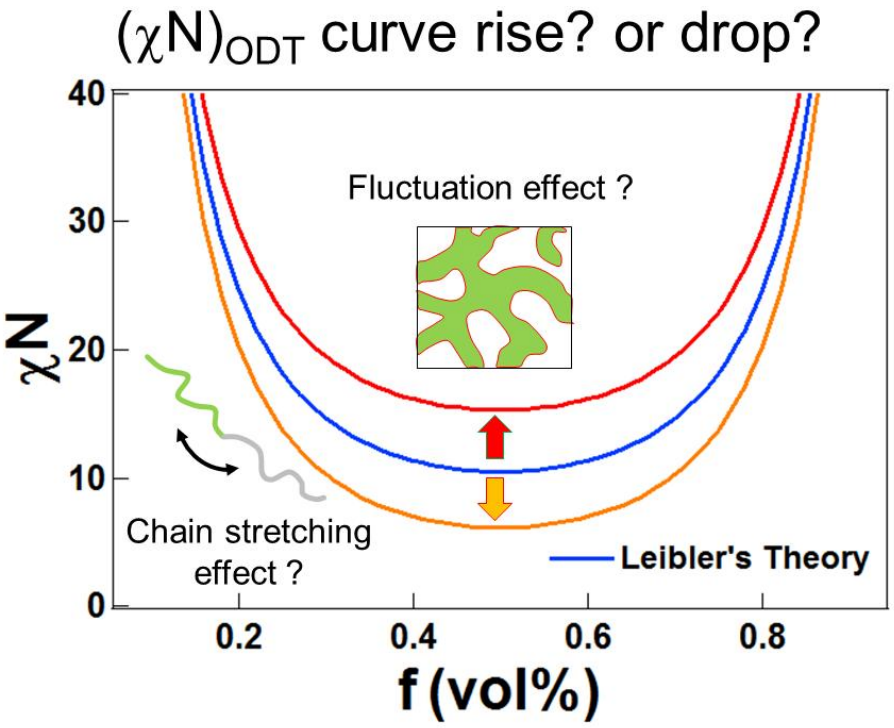

ABSTRACT: The phase behavior in relatively low-molecular-weight poly(ε-caprolactone)-poly(butadiene) diblock copolymers (PCL-PB) were investigated using small angle X-ray scattering (SAXS). The temperature dependence of χ was determined from the curve fitting of SAXS profiles using random phase approximation in the disordered state. The phase diagram for PCL-PB was constructed. Generally, according to Fredrickson-Helfand theory, the product $(\chi N)_{ODT}$, where N is the degree of polymerization and χ is the Flory-Huggins interaction parameter at the order-disorder transition temperature, is considered to be shifted toward upper side in phase diagram due to the existence of fluctuation. However, in PCL-PB, the significant increase of $(\chi N)_{ODT}$ was not apparently observed. In order to compare $(\chi N)_{ODT}$ values with theoretical and many experimental studies, we calculated $(\chi N)_{ODT}$ which was obtained from 19 earlier reports. We picked out 69 samples which formed lamellae morphology and had nearly symmetric composition. In the region of relatively low-molecular-weight, it was found that the increase of $(\chi N)_{ODT}$ was not clearly seen in the almost all of investigated articles.

KEY WORDS block copolymer / order-disorder transition / fluctuation

1. INTRODUCTION

Block copolymers have received considerable attention from both academic and industrial perspectives for decades. When repulsive force works between constituent blocks, long-ranged ordered structures with periodicity in nanometer scale are self-assembled [1-3]. These ordered structures reported to date are spheres arranged in body-centered cubic lattice (BCC), hexagonally packed cylinders (HEX), gyroid (Gyr) and lamellar structure (LAM). Recently, *Fddd* structure which is orthorhombic lattice and single network morphology [3,4] and Frank-Kasper sigma phase which has $P4_2/mnm$ symmetry and 30 spheres in a unit cell were discovered [5]. The morphology is predicted by χN and f (χ is the Flory-Huggins interaction parameter, N is the total degree of polymerization and f is the volume fraction of one block).

Phase behavior of block copolymer has been extensively studied both theoretically and experimentally. Leibler formulated the phase behavior in weakly segregated limit by a random phase approximation (RPA) [6]. Using a RPA method, he computed the spectrum of composition fluctuations in disordered state, and used Landau type mean field approximation to estimate the location of the ODT and nature of the ordered state as a function of composition. In this theory, it is possible to directly transform from disordered state to ordered lamellar phase at only $f = 0.5$. The order-disorder transition (ODT) at $f = 0.5$ is the second order transition, while ODT at $f \neq 0.5$ is the first order. Leibler pointed out that the Landau theory which predicts mean field critical behavior is inadequate in $f = 0.5$ critical

point. Brazovskii had reported that such critical point is suppressed by large amplitude order parameter fluctuation. Fredrickson and Helfand extended Brazovskii's Hartree method [7] and implemented fluctuation effects (so called Brazovskii's effects) in correcting Leibler's mean field theory [8]. Fredrickson-Helfand theory (FH theory) identifies ODT as a fluctuation-induced weak first order transition. Moreover, transformation from disordered state to ordered state can occur directly at $f \neq 0.5$. There has been considerable experimental research on ODT. These studies showed that ordered states transformed directly from disordered state, supporting that FH theory is correct [1,2,9]. Leibler's mean field theory also predicts that the reciprocal scattering intensity (I_m^{-1}) changes linearly with $1/T$ in disordered state, but I_m^{-1} appeared to deviate from the linear relation near ODT in many experimental results. This can be also accounted for in terms of the temperature window where fluctuation exist according to FH theory. At high enough temperatures above the order-disorder transition temperature (T_{ODT}), fluctuation effects diminish, and this temperature range can be described by Leibler's mean field theory. The crossover temperature and χN from mean-field type to non-mean-filed type are designated as T_{MF} and $(\chi N)_{MF}$, respectively. There appear to be two regimes in the disordered state; (i) $T_{ODT} < T < T_{MF}$, composition fluctuation exists, and the density of constituent monomer is not uniform. (ii) $T > T_{MF}$, fluctuation effects diminish, and the density of constituent monomer is uniform [1,2,9].

FH theory also predicts that the order-disorder spinodal temperature shifts toward higher temperature in comparison to Leibler's theory. This shift in compositionally symmetric block copolymer

is dictated by following equation,

$$(\chi N)_{ODT} = 10.495 + 41.022\tilde{N}^{-1/3} \quad (1)$$

$$\tilde{N} = Na^6 v^{-2} \quad (2)$$

where a is the statistical segmental length, and v is the segmental volume. This equation is rigorously valid in $\tilde{N} > 10^9$. Since experimental values of $\tilde{N}$ generally range from 10^2 to 10^4, it is difficult to use actual block copolymer samples which has $\tilde{N}$ to satisfy eq. (1). Theoretical studies on phase behavior in relatively low-molecular-weight are mainly treated by Monte Carlo method [10-13]. In some results using Monte Carlo simulation, direct transformation from disordered to ordered state was observed, and χN at ODT, $(\chi N)_{\mathrm{ODT}}$, shifted to the upper side in the phase diagram [10,11]. One of the largest difference of order-disorder transition behavior between Leibler's and FH theory is that $(\chi N)_{\mathrm{ODT}}$ obtained from FH theory shifts toward upper side in phase diagram in comparison to Leibler's theory. In other word, the existence of fluctuation stabilizes disordered state.

The phase diagrams obtained experimentally for various systems were constructed, and compared with the one obtained from theory. For example, the phase diagram for polystyrene-polyisoprene block copolymer (PS-PI) [14,15], which is the most representative block copolymer in investigating the phase behavior, and poly(ethylene oxide)-poly(1,2-butylene oxide) block copolymer (PEO-PBO) [16], which are expected to be used for various applications, was experimentally obtained, serving as a guideline for synthesizing the block copolymers. To our knowledge, other than PS-PI and PEO-PBO, the phase

diagram for polyethylene−poly(ethylene-propylene) (PE-PEP) [9], poly(ethylene-propylene)−polyethylethylene (PEP-PEE) [9], polyethylene−polyethylethylene (PE-PEE) [17], poly(ethylene oxide)-polyisoprene (PEO-PI) [18], polylactide -poly(ethylene-alt-propylene) (PLA-PEP) [19], poly(DL-lactide)-poly(1,4-isoprene) (PLA-PI) [20], polystyrene−poly(2-vinylpyridine) (PS-P2VP) [21], polyoxyethylene-polyoxypropylene (POE-POP) [22] and poly(ethylene oxide)−poly(ethylethylene) (PEO-PEE)]23] had been constructed. The theoretical phase diagram is symmetric around f = 0.5, while the phase diagrams obtained from experiments were asymmetric around f = 0.5. This is due to the difference of size between constituent monomer, and the modified theory has been proposed [24]. Compared carefully within these phase diagrams, it can be realized that the behavior of $(cN)_{\mathrm{ODT}}$ line are roughly divided into two categories; one group whose $(cN)_{\mathrm{ODT}}$ curve apparently shifted toward upper side in phase diagram [14,17,18,21], and the other group indicated almost no shift [19,20,23]. In symmetric block copolymers, the absolute value of $(cN)_{\mathrm{ODT}}$ increases with a decreasing in molecular weight according to eq. (1). Although eq. (1) is strictly carried by $\tilde{N} > 10^9$, in some experimental reports, $(cN)_{\mathrm{ODT}}$ line appeared to shift upside in phase diagram despite using block copolymers with relatively low-molecular-weight [9,25]. In addition, it was reported that the temperature dependence of c was influenced by means of experimental method and analysis [26]. Therefore, it is difficult to determine c quantitatively. However, it is worthwhile to discuss qualitatively many experimental results of $(cN)_{\mathrm{ODT}}$ line in order to confirm the fluctuation effects.

There are a few studies on phase behavior in relatively low-molecular-weight block copolymers [19,20]. For example, in PLA-PEP system, the sample with N = 26 exhibits T_{ODT} = 159 ℃ [19]. In comparison to PS-PI where the sample with N = 203 shows T_{ODT} at 124 ℃ [14], phase separation in PLA-PEP could occur with smaller N. The chain dimension deviated from Gaussian statistics with smaller N, and hence it can be speculated that the phase behavior is different from that with larger N. However, it was reported that the phase behavior in relatively low-molecular-weight was similar to that in high molecular weight [19,20]. Recently, Matsen proposed that phase behavior in low-molecular-weight block copolymers modeled as freely jointed chain instead of Gaussian chain was investigated using self-consistent field theory (SCFT) [27]. In this theory, when the interfacial thickness is smaller than the bond length, $(\chi N)_{ODT}$ line is larger than $(\chi N)_{ODT}$ spinodal line predicted by Leibler's theory. Moreover, while the χ dependence of domain size D shows $D \sim \chi^{1/6}$ in usual Gaussian chain, the scaling changes to $D \sim \chi^{1/3}$ in freely jointed chain model.

Poly(ϵ-caprolactone)-poly(butadiene) block copolymer (PCL-PB) is a representative crystalline-amorphous block copolymer to investigate morphology depending on crystallization and melting behavior [29]. The temperature dependence of χ which is the most important parameter in block copolymer melts has not been determined for PCL-PB up to the present date. It is well known that the micro-phase separation occurs in PCL-PB with low molecular weight.

In this study, we report the phase behavior of PCL-PB block copolymers in order to reveal the

effects of low-molecular-weight. Our purpose is as follows; (i) to determine the temperature dependence of c for PCL-PB, and construct the phase diagram, (ii) to calculate $(cN)_{ODT}$ for PCL-PB, and compare it to the literatures data reported earlier. In relatively low-molecular weight block copolymer's systems, the increase of $(cN)_{ODT}$ arising from fluctuation was not clearly seen in the almost all of investigated articles. It was found that two factors, fluctuation and chain stretching effect, strongly influenced the location of $(cN)_{ODT}$ in low-molecular weight block copolymers.

2. EXPERIMENTAL SECTION

A series of PCL-PB were synthesized by anionic polymerization under high vacuum. Details of the polymerization procedure were reported previously [30]. The number -average molecular weight (M_n) of PB was determined by ^{1}H nuclear magnetic resonance (^{1}H-NMR). Heterogeneous index was measured by size exclusion chromatography (SEC) using PB standards. The volume fraction of PCL was calculated from ^{1}H-NMR. The molecular characteristics of the synthesized all 10 block copolymers are given in Table 1. The morphology was determined by SAXS. The total degree of polymerization (N) is defined by following equation

$$N = \frac{v_{PB}N_{PB} + v_{PCL}N_{PCL}}{\sqrt{v_{PB}v_{PCL}}} \qquad (3)$$

where v_{PB} and v_{PI} are the molar volume and taken to be 61.4 and 103.8 cm^3/mol, respectively [31]. N_{PB} and N_{PCL} are the degree of polymerization of PB and PCL, respectively. N is listed in Table 2. The

melting temperature (T_m) was determined from SAXS and defined as the temperature at which the temperature dependent SAXS invariant drastically changed in melting process, though all samples were not measured. The T_m of BCL2, BCL 3, BCL5 and BCL 10 were 55.2 ℃, 56.0 ℃, 56.8 ℃ and 60.6 ℃, respectively. The order-order transition temperature (T_{OOT}) was also determined from SAXS measurement and T_{OOT} between HEX and Gyr in BCL4 was 200 ℃.

Table 1. Molecular and morphological characteristics of diblock copolymers

code	$M_{n,PB}$ (g/mol)[a]	$M_{n,PB}$ (g/mol)[b]	M_w/M_n[c]	f_{PCL} (vol%)[a]	morphology[d]
BCL1	6400	1800	1.05	0.18	BCC
BCL2	5300	2200	1.06	0.24	HEX
BCL3	2800	1900	1.08	0.34	Gyr
BCL4	4500	3000	1.06	0.35	HEX/Gyr
BCL5	5400	4400	1.11	0.39	HEX
BCL6	2400	2000	1.19	0.39	Gyr
BCL7	3100	2700	1.09	0.41	LAM
BCL8	4200	3700	1.08	0.41	LAM
BCL9	2100	2100	1.08	0.45	LAM
BCL10	2800	4800	1.18	0.57	LAM

[a] Determined by ^{1}H-NMR.

[b] Determined by size exclusion chromatography (SEC) and ^{1}H-NMR.

[c] Determined by SEC.

[d] Determined by SAXS. Phase allocations are as follows: BCC, spheres arranged in body centered cubic lattice; HEX, hexagonally paced cylinders; Gyr, gyroid; LAM, lamellae.

Table 2. T_{ODT}, calculated N and $(cN)_{ODT}$ for PCL-PB

code	T_{ODT} (°C)	N	$(cN)_{ODT}$
BCL1	220	112	18.9
BCL2	200	100	17.4
BCL3	125	62	12.6
BCL4	Over 220	98	-
BCL5	Over 220	127	-
BCL6	110	57	12.0
BCL7	Over 220	75	-
BCL8	Over 220	101	-
BCL9	96	54	11.7
BCL10	Over 220	94	-

The small angle X-ray scattering (SAXS) measurements with synchrotron radiation were conducted at the beamline BL-9C in Photon Factory (PF) of High Energy Accelerator Research Organization in Tsukuba, Japan (KEK).The detector was a one-demensional position-sensitive proportional counter (PSPC) located at a distance of 1.0m. The energy of X-ray was 8.3 keV. Collagen (chicken tendon) was used as a standard specimen to calibrate SAXS detector. The scattering intensities were corrected for background scattering and sample absorption. The magnitude of scattering vector (q) is given by

$$q = \frac{4\pi}{\lambda}\sin\left(\frac{\theta}{2}\right) \qquad (4)$$

where λ is the wavelength of the X-ray and θ is the scattering angle. The sample temperature was controlled using Linkam LK-600 M (Japan Hightech). The sample was inserted into a sample cell which was sealed with polyimide film (12.5 mm thickness) windows at both sides. The thickness of sample cell is ca. 0.8 mm.

3. RESULTS AND DISCUSSION

3.1. Determination of order-disorder transition temperature

Fig. 1 shows SAXS profiles for BCL9 in heating process. The thermal history was as follows; measurements were made at intervals 4 °C on heating process. The sample was held for 10 min at the target temperature and a measuring time was 1 min. Just before accumulating the data, an X-ray was not

irradiated to the sample to avoid the X-ray damage and the local heating of sample due to high-intensity synchrotron beam. Since the thickness of the sample cell was just ca. 0.8 mm and the sample had been kept at each temperature for 10 min, it was considered that the temperature gradient in sample was fully eliminated. In our earlier work, we reported that relaxation of PCL-PB chains which has almost the same molecular weight in this paper was identified in the case of 2 °C / min heating rate [32]. Therefore, in this report, it was considered that the system reached substantially equilibrium state. It can be seen in Fig. 1 that the scattering intensity started decreasing drastically at 96 °C. Above 104 °C, the scattering profiles show only one broad peak with small scattering intensity that is ascribed to the scattering from correlation hole in disordered phase of block copolymer.

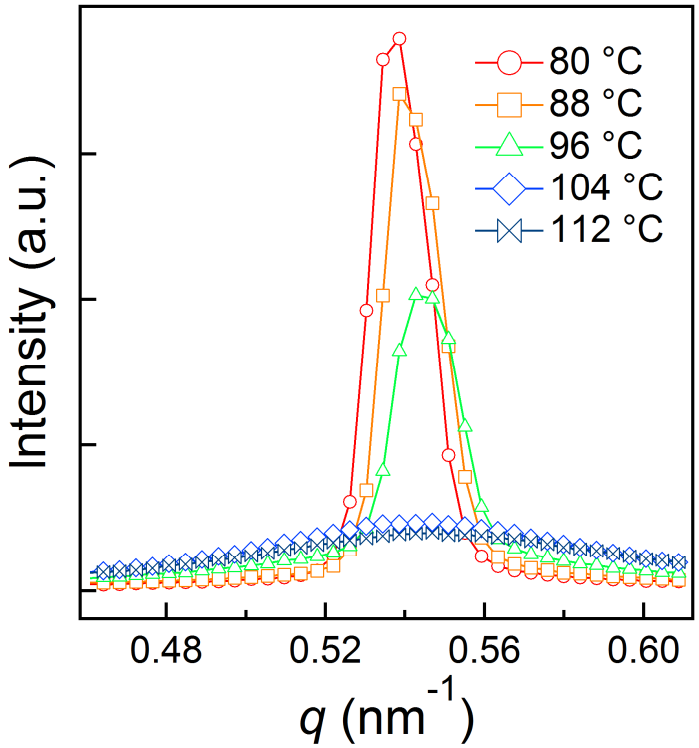

FIG. 1. Temperature dependence of SAXS profiles for BCL9 in heating process.

In order to determine the order-disorder transition temperature (T_{ODT}), the reciprocal of maximum scattered intensity ($1/I_m$) and the square of half-width at half maximum (s_q^2) versus the reciprocal of absolute temperature ($1/T$) during heating and cooling process are shown in Fig. 2. In the cooling process, the sample was cooled from 200 °C to 100 °C under the same thermal condition in heating process. Both $1/I_m$ and s_q^2 showed discontinuous change at 96 °C. This temperature is defined as T_{ODT}, and hence it was found that T_{ODT} was 96 °C. When the sample was heated above 168 °C, both $1/I_m$ and s_q^2 changed linearly with increasing temperature. According to Leibler's mean field theory, the linear relation of both $1/I_m$ and s_q^2 with $1/T$ is observed in disordered state. On the other hand, FH theory predicts that $1/I_m$ appears to deviate from the linear relation in the temperature window where fluctuation exists. The crossover temperature (T_{MF}) above which fluctuation effects become less significant and mean field theory becomes a good approximation was over 168 °C. The T_{ODT} s of other samples were listed in Table 2.

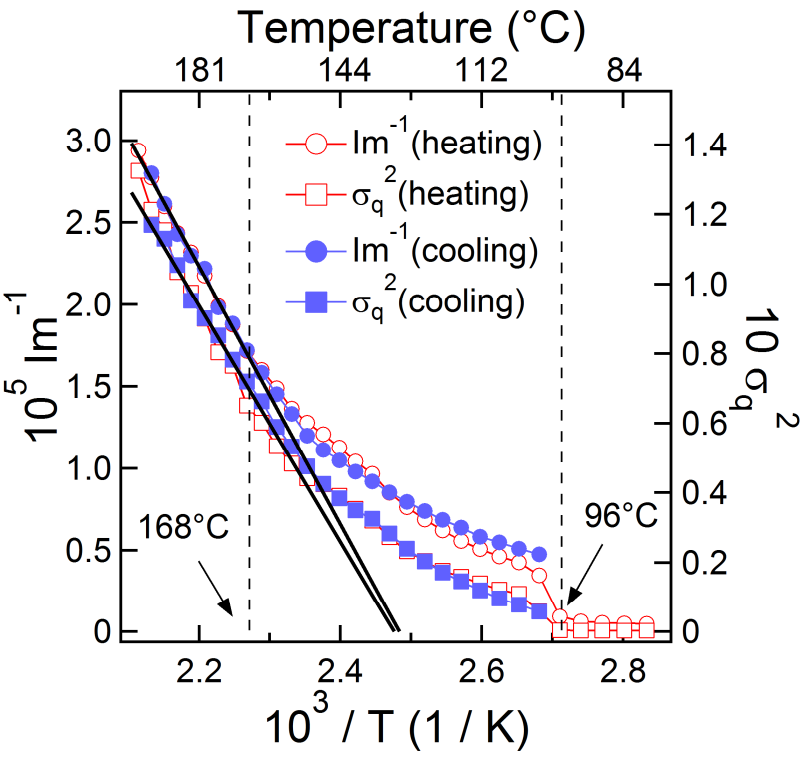

FIG. 2. I_m^{-1} (Inverse of the scattered intensity at q^*) and s_q^2 (square of full-width at half-maximun at q^*) plotted as a function of $1/T$ for BCL9 in heating and cooling process, where q^* is the q-value at the first-order scattering maximum.

The characteristic length D is given by

$$D = \frac{2p}{q^*} \qquad (5)$$

where q^* is the position of the maximum peak in SAXS profiles. Fig. 3 shows plots of D obtained in disordered state versus $1/T$. The temperature dependence of D in disordered state has been reported by various research gropes, but the behavior of D was diverse by reports. Stuhn et al. [33] reported that the

temperature dependence of D showed discontinuous change across T_{ODT}, while Lee et al. [20], Bates et al. [34], Hashimoto et al. [35], Rosedale et al. [36] and Almdal et al. [37] could not find the discontinuity around T_{ODT}. Additionally, Wolf et al. [38] found that the temperature dependence of D slightly changed at T_{MF}, but Hashimoto et al. [39] and Bates et al. [36] reported no change of D across T_{MF}. On the other hand, in Monte Carlo simulations, q^* changes continuously throughout T_{ODT} [10,11]. In our results, it was found that the temperature dependence of D showed no change at both T_{ODT} (96°C) and T_{MF} (168°C) as shown in Fig. 3.

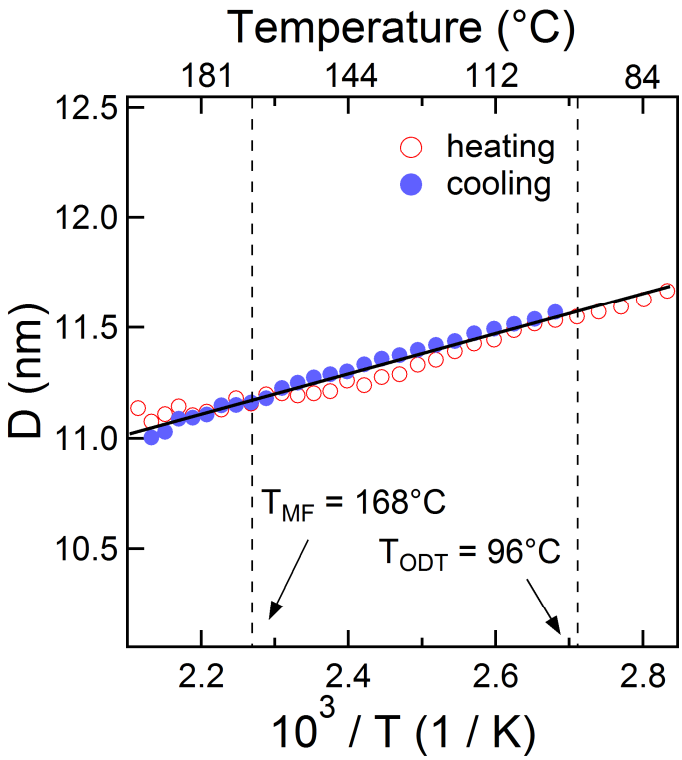

FIG. 3. Characteristic length D (=2p/q*) plotted as a function of 1/T.

3.2. Determination of the temperature dependence of c and construction of phase diagram for PCL-PB

The temperature dependence of c can be estimated by analyzing SAXS profiles in disordered state on the basis of Leibler's mean-field theory [6]. In the context of mean-field theory, the structure factor for homogeneous block copolymer is given by the general expression

$$I(q) = N / [F(x) - 2cN] \tag{6}$$

with

$$F(x) = g_1(1,x) / \{ g_1(f,x) g_1(1-f,x) / 4[g_1(1,x) - g_1(f,x) - g_1(1-f,x)]^2 \} \tag{7}$$

$$g_1(f,x) = 2[fx + \exp(-fx) - 1] / x^2 \tag{8}$$

$$x = \frac{q^2 N a^2}{6} = q^2 R_g^{\ 2} \tag{9}$$

where a is the statistical segmental length, and R_g is the radius of gyration of block copolymer chain [6]. The SAXS profiles obtained from experiments and theoretical curves using eq. (6) are shown in Fig. 4.

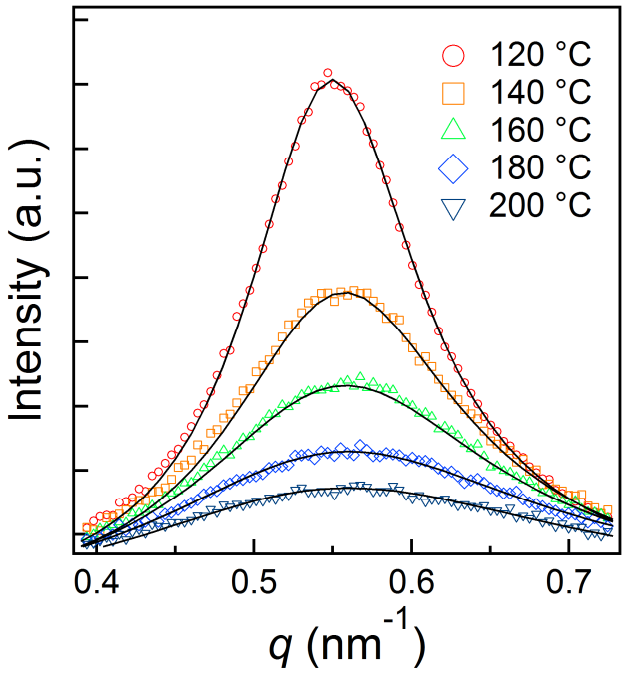

FIG. 4. Best fits between experimental and theoretical scattering profiles for BCL9 at 120, 140, 160, 180

and 200 °C. The solid curves are calculated scattering profiles using eq. (6).

SAXS profiles obtained experimentally were in almost good agreement with theoretical curves. Fig. 5 shows the c values extracted from the analyzed SAXS data versus $1/T$. The linear least-squares fit yields

$$c = -0.0229 + 71.65/T \qquad (10)$$

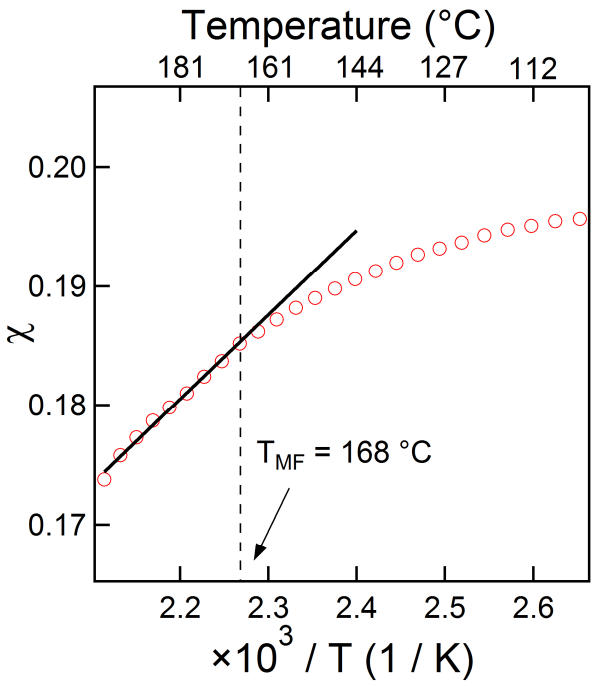

FIG. 5. The temperature dependence of c obtained from eq. (6) for BCL9.

In the Leibler's theory, block copolymer chains in disordered state are hypothesized to be Gaussian statistic, characterized by an unperturbed radius of gyration that scales as $R_g \sim N^{1/2}$. It follows that the peak wave vector q^* in the fluctuation spectrum is predicted to scales as $q^* \sim R_g \sim N^{1/2}$. FH theory retained these features of the traditional RPA. However, from various results of experiments and

simulations, it was reported that polymer chains in disordered state are stretched coil rather than Gaussian coil [9-13,26,34]. The value of R_g anticipated unperturbed Gaussian coil is defined by

$$Rg = \left(\frac{a_{PCL}^{\,2} N_{PCL} + a_{PB}^{\,2} N_{PCL}}{6} \right)^{1/2} \qquad (11)$$

With values of a_{PCL} = 0.82 nm [40] and a_{PB} = 0.69 nm [41], we obtained R_g = 2.46 nm. On the other hand, R_g obtained by fitting SAXS profile at 96 °C using eq. (6) was 3.28 nm, which was about 33 % larger than the one obtained by eq. (11). This result indicates that polymer chains in disordered state was stretched more than unperturbed chain. In PE-PEP [26] and PEP-PEE [36], R_g in disordered state obtained by experiment was about 18 % and 31 % larger than Gaussian chain, respectively. In Monte Carlo simulations, R_g in disordered state is about 1.25 times larger than Gaussian coil [10,11]. Therefore, our results were almost coincident with early works. In some Monte Carlo simulations, there is a discrepancy between increase of R_g and decrease of q^* as χN increases from zero to $(\chi N)_{\mathrm{ODT}}$ [10,11]. As some theoretical researchers have pointed out, this implies that the shift of q^* is not simply chain stretching, but a cooperative (or collective) organization of the molecules [11]. A thorough discussion of this discrepancy is beyond the scope of present study.

The phase diagram for PCL-PB is illustrated in Fig. 6. The filled circles on the diagram denote ODT, and open square represents order-order transition. Thick solid lines indicate the χN ranges of the ordered phases and thin solid lines represent the phase boundary. The dashed line is a spinodal line calculated from eq. (6).

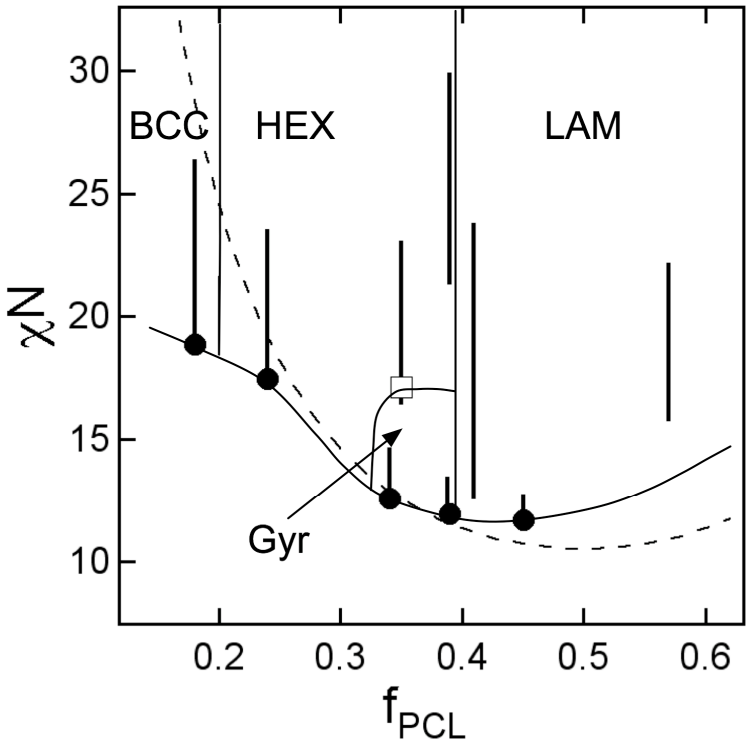

FIG. 6. Experimentally obtained PCL-PB phase diagram. Solid circles indicate the order-disorder transition determined by SAXS. Open square indicates order-order transition. The solid line is drawn to indicate the different boundary. Thick vertical lines show the range of χN explored by SAXS for each samples. The dashed line is a spinodal line predicted by using eq. (6). Phase notation is as follows: LAM, lamellae; Gyr, gyroid; HEX, hexagonally packed cylinders; BCC, spheres arranged in body centered cubic lattice.

The ordered microstructure observed were lamellae (LAM), gyroid (Gyr), hexagonally packed cylinders

(HEX) and spheres arranged in body centered cubic lattice (BCC), which are similar to those reported for common block copolymers. The $(\chi N)_{ODT}$ curve obtained experimentally was located near spinodal curve, $(\chi N)_{ODT,s}$, which was derived from Leibler's theory. This feature resembles PEP-PLA [19] and PI-PLA [20] systems. In the compositional range $f_{PCL} < 0.24$, $(\chi N)_{ODT}$ was lower than $(\chi N)_{ODT,s}$. According to FH theory, since disordered state is stabilized in the presence of fluctuation, $(\chi N)_{ODT}$ shifts upward from $(\chi N)_{ODT,s}$ [1,2,9]. In symmetric block copolymer, the shift amount decreases as a molecular weight increases according to eq. (1). Note that eq. (1) is only rigorously accurate at very large of $\tilde{N}$ ($>10^9$). Since experimental values of $\tilde{N}$ range from 10^2 to 10^4, eq. (1) generally seems to be practically inapplicable in almost experimental results. Theoretically, Monte Carlo simulations are often used to treat realistic $\tilde{N}$. Some research groups using Monte Carlo method reported that $(\chi N)_{ODT}$ is larger than $(\chi N)_{ODT,s}$ [10-13]. Recently, the SCFT jointed together with freely jointed chain model predicted that $(\chi N)_{ODT,s}$ increases in itself with decreasing N [27]. When experimental phase diagrams of various block copolymer systems were compared carefully, one can realize that the $(\chi N)_{ODT}$ line are roughly divided into two categories; one group whose $(\chi N)_{ODT}$ curve apparently shifted toward upper side in phase diagram [14,17,18,21], and the other group indicated almost no shift [19,20,23]. The common characteristics of the latter group were that all block copolymers had relatively smaller molecular weight as compared with the former group. Since $(\chi N)_{ODT}$ shifts upward from $(\chi N)_{ODT,s}$ as decreasing $\tilde{N}$ theoretically, the latter group including our PCL-PB results were different from theoretical ones. Besides,

in PEP-PLA [19] and PLA-PI [20], which had almost the same $\tilde{N}$ values for PCL-PB, it was also observed that the $(\chi N)_{ODT}$ line obtained experimentally was partially smaller than theoretical ones. In the highly asymmetric composition region for PLA-PI, $(\chi N)_{ODT}$ was lower than $(\chi N)_{ODT,s}$, and hence these results were coincident with our PCL-PB. Therefore, it must be closely examined whether existence of fluctuation actually influences $(\chi N)_{ODT}$ or not. We discuss this effects in details in the next section.

The asymmetry of the phase diagram could be accounted for by the conformational asymmetry, $\varepsilon = v_A a_A^2/(v_B a_B^2)$. Generally, the larger the conformational asymmetry is, the more the phase diagram skews all the boundary lines dividing ordered phases to one side of the phase diagram [9,24]. In order to confirm the availability of ε, the composition range of the gyroid phase was often discussed or the phase diagram itself was directly compared with different systems. The PCL-PB system exhibited relatively high $\varepsilon_{PCL\text{-}PB} \sim 2.4$, and the extent of gyroid phase was obtained for $0.34 < f_{PCL} < 0.39$. The PCL-PB system values should be compared with the previously reported cases with $\varepsilon_{PS\text{-}P2VP} \sim 1$ [21], $\varepsilon_{PS\text{-}PI} \sim 1.5$ [14], $\varepsilon_{PEP\text{-}PEE} \sim 1.7$ [9], $\varepsilon_{PE\text{-}PEE} \sim 2.5$ [17] and $\varepsilon_{PEO\text{-}PI} \sim 2.7$ [18]. In these systems, the gyroid phases were observed in the range of $0.35 < f_{PS} < 0.4$, $0.35 < f_{PS} < 0.4$, $0.38 < f_{PEP} < 0.42$, $0.37 < f_{PE} < 0.43$ and $0.4 < f_{PEO} < 0.45$, respectively. In comparison with these values, while $\varepsilon_{PCL\text{-}PB}$ was relatively large, the extent of gyroid of the PCL-PB was roughly similar to that of the PS-P2PV with $\varepsilon \sim 1$, and hence there was a discrepancy between the PB-PCL system in our experiment and the earlier experimental and theoretical works. However, it was reported that the phase diagram does not vary simply with ε [42].

Since significant difference in the window of gyroid region was found in PCL-PB as compared with both various systems and theory, the parameters, f, χN and ε are not sufficient to completely describe block copolymer phase diagram.

3.3. Comparison of $(\chi N)_{ODT}$ to literature values

As mentioned in the previous section, $(\chi N)_{\mathrm{ODT}}$ line obtained in the PCL-PB was located near and partially smaller than Leibler's theoretical one. According to FH theory and many Monte Carlo simulations, $(\chi N)_{\mathrm{ODT}}$ becomes large with decreasing N, and hence our results were in contradiction to the theoretical works. In order to compare $(\chi N)_{\mathrm{ODT}}$ values with many experimental studies including our PCL-PB, we calculated $(\chi N)_{\mathrm{ODT}}$ which was obtained in many earlier reports. We picked out samples which formed lamellae morphology and had nearly symmetric composition. Eventually, we used in total 20 reports including this paper (15 block copolymer's system) and 69 sample, showing a summary of characteristic of the block copolymers in Table 3. The volume fraction of samples represents for the component designated in front of sample code name. For example, in PS-PI, f listed in Table 3 means PS vol%. Table 4 gives a summary of the temperature dependence of χ used to calculate $(\chi N)_{\mathrm{ODT}}$ and the experimental method employed. Fig. 7 shows the plot of $(\chi N)_{\mathrm{ODT}}$ / $(\chi N)_{\mathrm{ODT,s}}$ -1 versus $\tilde{N}$. The numbers in brackets in explanatory for legend symbols stand for to the reference numbers. The solid line was obtained by a theoretical calculation from eq. (1). If $(\chi N)_{\mathrm{ODT}}$ obtained from experiments is similar to the

Leibler's theory, the value of $(cN)_{ODT}$ / $(cN)_{ODT,s}$ -1 approaches to zero.

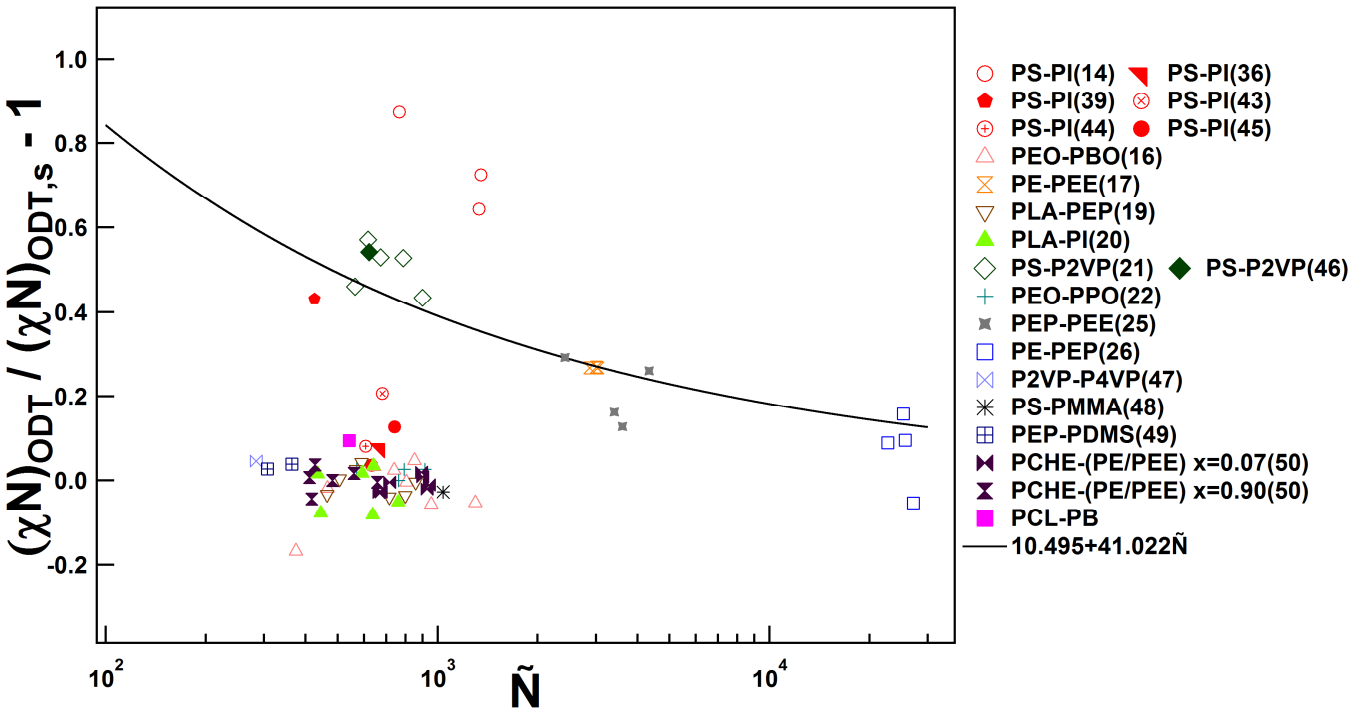

FIG. 7. The plots of $(cN)_{ODT}$ / $(cN)_{ODT,s}$ -1 versus $\tilde{N}$. The solid line represents theoretical curve predicted by using eq. (1). Detailed data is listed in Table 3. The numbers in brackets correspond to reference number.

It can be seen in Fig. 7 that experimental results were almost consistent with FH theory in $\tilde{N} > 10^3$, even though only three systems were applied (PE-PEE, PEP-PEE and PE-PEP). The samples in the range in $10^2 < \tilde{N} < 10^3$ can be divided into two categories; one is $(cN)_{ODT}$ / $(cN)_{ODT,s}$ -1 ~ FH theory (on the solid line in Fig. 7) , and the other is $(cN)_{ODT}$ / $(cN)_{ODT,s}$ -1 ~ 0.The former group contained PS-P2VP and a part of PS-PI, and the rest showed $(cN)_{ODT}$ /$(cN)_{ODT,s}$ -1 ~ 0.

In PS-PI system, although there were six reports, two articles of ref. 14 and ref. 39 nearly lay on the FH theory. The temperature dependence of χ used in ref. 14 and ref. 39 was obtained by means of turbidity method, while the others were determined by small angle scattering and rheology methods. The temperature dependence of χ obtained from scattering and rheology methods is almost coincident with each other. But those obtained from turbidity have a large margin of error, implying overestimation of temperature dependent χ. On the other hand, in PS-P2VP, two different research groups obtained almost the same result by scattering method, and hence these results seem to be reliable. Here, let us have a look at some systematic subject such as chemical nature of the block copolymers or systematic experimental techniques (e.g., SAXS, SANS, or rheology) used by each report in Fig. 7. In PS-P2VP system, in which each temperature dependent χ was determined by different techniques (rheology in ref. 21 and SAXS in ref. 46), the values of $(\chi N)_{ODT}$ / $(\chi N)_{ODT,s}$ -1 are almost coincidence with each other. As for chemical nature of the block copolymers, there was not a significant difference between hydrocarbon block copolymer, such as PCHE-(PE/PEE) in ref. 50, and block copolymers which have polar molecules in one block component, such as PLA-PEP in ref. 19. In PEO-PPO (ref. 22) and P2VP-P4VP (ref. 47), in which have polar molecules in both blocks, significant differences of $(\chi N)_{ODT}$ / $(\chi N)_{ODT,s}$ -1 were not also seen. Within the scope of our investigation, the significant difference of $(\chi N)_{ODT}$ / $(\chi N)_{ODT,s}$ -1 was not observed between chemical nature and experimental techniques used in Fig. 7 except for PS-P2VP chemical system and turbidity experimental method.

In the range of $10^2 < \tilde{N} < 10^3$, except for PS-PI in ref. 13 and ref. 37 and PS-P2VP, it was found that the rest of 13 articles results was in disagreement with the FH theory. As mentioned above, though FH theory rigorously cannot be applicable to actual block copolymers in accordance with eq. (1), it was experimentally observed that $(\chi N)_{ODT}$ is higher than $(\chi N)_{ODT,s}$ in some reports [1,2,9]. Additionally, many Monte Carlo simulations also confirmed that $(\chi N)_{ODT}$ is larger than $(\chi N)_{ODT,s}$ [10-12]. Therefore, the 13 results presented in Fig. 7 were in contradiction to these earlier works. It is well known that polymer chains in disordered state take stretched coils as a favorable conformation rather than Gaussian coils. The improved mean filed theory that accommodates chain stretching proposed by Mauror et al. indicates that $(\chi N)_{ODT,s}$ is smaller than one derived from the Leibler's theory with strengthening chain stretching [26]. According to this theory, for example, when chains are 18% larger than Gaussian chain, $(\chi N)_{ODT}$ is located at 7.34. On the other hand, as already described above, the existence of fluctuation stabilizes disordered state, leading to the increase of $(\chi N)_{ODT}$. Therefore, we speculate that $(\chi N)_{ODT}$ drops to lower side in a phase diagram due to the effect of chain stretching, while $(\chi N)_{ODT}$ rises because of the existence of fluctuation. For these reasons, in the range of $10^2 < \tilde{N} < 10^3$, these two factors compete each other, and then consequently the significant increase of $(\chi N)_{ODT}$ could not be observed. On the other hand, in the case of high molecular weight, due to relaxation of chain stretching, decrease of $(\chi N)_{ODT}$ which is attributable to chain stretching was not seen, and thus $(\chi N)_{ODT}$ was located at near FH theory. If the chain stretching effect is implemented in FH theory, these results might be explained. Since

$(\chi N)_{ODT}$ in the case of PS-P2VP was located close to FH theory, factors other than f, χN and fluctuation might influence the location of$(\chi N)_{ODT}$.

In the previous section, we mentioned that $(\chi N)_{ODT}$ line in the highly asymmetric composition region of PCL-PB was lower than $(\chi N)_{ODT,s}$. In this paper, we focused on the samples which formed lamellar morphology and had nearly symmetric composition. In the systems of PEP-PLA, PLA-PI and PCL-PB, $(\chi N)_{ODT}$ deviated from $(\chi N)_{ODT,s}$ as being highly asymmetric. The composition may also influence to the location of $(\chi N)_{ODT}$, but a discussion of this effect is beyond the scope of this paper.

Essentially, we should compare directly $(\chi N)_{ODT}$ in the same block copolymer's system. However, in an experimental matter, a molecular weight of synthesized samples cannot be changed to be much larger in order to observe the order-disorder transition in an available experimental temperature range. Thus, it is difficult to compare $(\chi N)_{ODT}$ directly within the same system. As shown in Fig. 7, in $N > 10^3$, $(\chi N)_{ODT}$ increased with decreasing N. On the other hand, in $10^2 < N < 10^3$, the increase in $(\chi N)_{ODT}$ was not clearly seen. No significant increase of $(\chi N)_{ODT}$ was observed in relatively low molecular weight block copolymers by referring various systems that had a wider range of molecular weight, although it is difficult to compare $(\chi N)_{ODT}$ directly in the same system.

~~Though it is difficult to compare $(\chi N)_{ODT}$ directly in the same system, by investigation of various systems which had wider range of molecular weight, we considered that the significant increases of $(\chi N)_{ODT}$ could not be observed in relatively low molecular weight block copolymers.~~

Recently, the SCFT using freely jointed chain model, which even provides a reasonable model for low molecular weight polymers or surfactant, was proposed [27]. As mentioned above, according to this new theory, $(cN)_{ODT,s}$ becomes larger than the one derived from the Leibler's theory as decreasing N. This freely jointed chain model is only available for short chain length $N < 200$ and/or strong interaction $c > 0.2$. In our PCL-PB study, because of $c = 0.23$ at 80 °C using eq. (10), it is suitable to confirm whether this model is appropriate for low-molecular-weight block copolymers or not. Judging from c values at T_{MF} using the temperature dependence of c listed in Table 3, it was found that PEP-PLA, P2VP-P4VP, PI-PLA and PCL-PB systems satisfied $c > 0.2$ which is the requirement applicable to freely jointed chain model. As can be seen in Fig. 7, though these systems existed in $10^2 < \tilde{N} < 10^3$, the increase of $(cN)_{ODT}$ was not apparently observed. Therefore, this model could not be applied to our results. This is attributed to the existence of molecular weight distribution in our samples. Since much shorter chains are mixed near interface of domains, it can be easily considered that the thickness of interface becomes larger than bond length. These results indicate that since relatively low molecular weight systems investigated in this paper have diffuse interface, the chain stretching is not ascribed to the strong segregation limit system. As described above, this chain stretching is attributed to the low-molecular-weight. If the molecular weight distribution in the sample would be taken into account in this new theory, this model could be refined and reflect accurate results.

Table 3. Summary of the molecular characteristics of various block copolymers

code	code	f (vol%)	N	T_{ODT} (°C)	Ref.
PS-PI	IS-54	0.46	203	124	14
	IS-42	0.58	355	250	
	IS-41	0.59	360	239	
	SI 6/8	0.38	180	70	36
	SI 5/5	0.46	119	41	39
	OSI-3	0.45	180	100	43
	SI	0.5	161	85	44
	SI-R	0.51	177	100	45
	SI-X	0.46	180	120	
PEO-PBO	E43B23	0.5	86	43	16
	E85B45	0.5	170	140	
	E100B51	0.51	196	165	
	E56B27	0.52	107	53	
	E76B38	0.51	148	109	
	E96B47	0.52	185	163	
	E114B56	0.52	220	210	

	E155B76	0.52	299	270	
PE-PEE	8H	0.5	427	136	17
	3D	0.49	407	120	
	18H	0.47	610	276	
PLA-PEP	2	0.5	26	159	19
	3	0.54	28	163	
	4	0.58	31	170	
	12	0.51	34	180	
	13	0.5	40	226	
	14	0.55	44	236	
	15	0.57	47	238	
PLA-PI	IL-1	0.51	39	93	20
	IL-2	0.54	49	110	
	IL-3	0.54	63	153	
	IL-7	0.56	51	111	
	IL-10	0.5	57	146	
	IL-11	0.4	48	98	
PS-P2VP	SV-20	0.5	143	180	21

	SV18	0.5	200	250	
	SV19	0.5	229	297	
	SV-17	0.5	171	212	
	SV-15	0.5	157	185	
	S2VP-2	0.52	173	154	46
PEO-PPO	E91P64	0.49	186	80	22
	E128P82	0.51	249	128	
	E135P84	0.52	259	130	
	E144P105	0.48	299	150	
PEP-PEE	14H	0.54	761	16	25
	2H	0.56	895	96	
	5H	0.55	978	125	
	3H	0.53	1451	291	
PE-PEP	PE-PEP-1D	0.5	1570	119	26
	PE-PEP-2H	0.49	1920	139	
	PE-PEP-3D	0.49	2290	159	
	PE-PEP-6H	0.5	1930	139	
P2VP-P4VP	P24VP-L	0.56	57	266	47

PS-PMMA	sample1	0.56	277	203	48
PEP-PDMS	PEP-PDMS 6	0.48	106	64	49
	PEP-PDMS 17	0.5	148	165	
PC-(PE/PEE) x=0.07	1	0.54	210	168	50
	2	0.55	216	172	
	3	0.54	223	180	
	4	0.52	257	227	
	5	0.53	266	234	
	6	0.52	269	250	
	7	0.53	277	263	
PC-(PE/PEE) x=0.9	38	0.48	618	184	
	39	0.5	635	177	
	40	0.5	660	180	
	41	0.51	760	236	
	42	0.5	864	273	
	43	0.5	1015	335	

PCL-PB	BCL9	0.45	54	96	-

Table 4. Summary of interaction parameter reported in the literature for various block copolymers

code	Ref.	Temperature dependence of c	Method employed
PS-PI	14	c = -0.0857+71.4/T	turbidity
	36,45	c = -0.0419+38.5/T	SAXS
	39	a = -0.00118+0.839/T^a	turbidity
	43	c = -0.0197+34.1/T	SAXS
	44	c = -0.079+54/T	rheology
PEO-PBO	16	c = -0.0617+51.6/T	SAXS
PE-PEE	17	c = -0.0055+15/T	SAXS
PLA-PEP	19	c = -0.64+445/T	rheology
PLA-PI	20	c = -0.38+29.4/T	rheology
PS-P2VP	21	c = -0.095+91.6/T	rheology
	46	a = -1.79×10^{-4}+0.478/T^a	SAXS
PEO-PPO	22	c = -0.122+66.8/T	SAXS
PEP-PEE	25	c = 0.0015+51.6/T	rheology

PE-PEP	26	c = -0.029+14.4/T	SANS
P2VP-P4VP	47	a = 1.64×10^{-3}+0.236/T[a]	SAXS
PS-PMMA	48	c = 0.0282+4.46/T	SAXS
PEP-PDMS	49	c = -0.0209+41.4/T	SAXS
PC-(PE/PEE)x=0.07	50	c = -0.0175+29.4/T	rheology
PC-(PE/PEE)x=0.9	50	c = -0.0078+11/T	rheology
PCL-PB	-	eq. (10)	SAXS

[a] a is related to c by $c = a\ V_{ref}$, V_{ref} being the molar volume of a reference component

4. CONCLUSIONS

The phase behavior and fluctuation effects in synthesized PCL-PB (10 samples) were investigated by SAXS. The temperature dependence of c was estimated by analyzing the SAXS profiles on the basis of the Leibler's theory. We obtained the temperature dependence of c for the PCL-PB as c = -0.0229 + 71.65/T. The temperature dependence of D showed no change at both T_{ODT} and T_{MF}. The R_g obtained by RPA fitting SAXS profile in disordered state was 3.28 nm, which was about 33 % larger than the one obtained by usual Gaussian statics. The phase diagram for the PCL-PB was constructed using the

temperature dependence of χ. The phase diagram consists of four ordered phases: LAM, Gyr, HEX and BCC. Although $\varepsilon_{PCL\text{-}PB}$ is relatively large in comparison with common block copolymers, the extent of Gyr was roughly similar to that of the common block copolymers with $\varepsilon \sim 1$. It was also observed that $(\chi N)_{ODT}$ curve obtained experimentally was located near spinodal curve derived from the Leibler's theory. In order to compare $(\chi N)_{ODT}$ values with theoretical and many experimental studies, we calculated $(\chi N)_{ODT}$ which was obtained from 19 earlier reports. We picked out 69 samples which formed lamellae morphology and had nearly symmetric composition. In $\tilde{N} > 10^3$, the experimentally obtained $(\chi N)_{ODT}$ were almost consistence with the FH theory. On the other hand, in $10^2 < \tilde{N} < 10^3$, the increase in $(\chi N)_{ODT}$ was not clearly seen in almost all of investigated articles. This is attributed to two factors, composition fluctuation and chain stretching effect. The $(\chi N)_{ODT}$ line rises to upper side in a phase diagram due to the existence of fluctuation, while $(\chi N)_{ODT}$ drops to lower side because of the effect of chain stretching arising from low-molecular weight. These two factors compete each other, and then consequently the significant increase of $(\chi N)_{ODT}$ could not be observed. In the case of high-molecular weight, the decrease of $(\chi N)_{ODT}$ is not seen due to relaxation of chain stretching effect.

ACKNOWLEDGMENT

The SAXS measurement was performed under approval of the Photon Factory Program Advisory Committee (Proposal No. 2005G245, 2006G342, and 2008G525).

REFERENCES

[1] Bates FS, Fredrickson GH, Annu Rev Phys Chem 1990;41:525-57.

[2] Kim JK, Han CD, Adv Polym Sci 2010;231:77-145.

[3] Meuler AJ, Hillmyer MA, Bates FS, Macromolecules 2009;42:7221-50.

[4] Kim MI, Wakada T, Akasaka S, Nishitsuji S, Saijo K, Hasegawa H, Ito K, Takenaka M, Macromolecules 2009;42:5266-71.

[5] Lee S, Bluemle MJ, Bates FS, Science 2010;330:349-353.

[6] Leibler LW, Macromolecules 1980;13:1602-17.

[7] Brazovskii S, Soviet Phys JETP 1975;41:85-9.

[8] Fredrickson GH, Helfand E, J Chem Phys 1986;87:697-705.

[9] Bates FS, Schulz MF, Khandpur AK, Forster S, Rosedale JH, Almdal K, Mortensen K, Faraday Discuss1994;98:7-18.

[10] Fried H, Binder K, J Chem Phys 1991;94:8349-66.

[11] Vassiliev ON, Matsen MW, J Chem Phys 2003;118:7700-13.

[12] Matsen MW, Griffiths GH, Wickham RA, Vassiliev ON. J Chem Phys 2006;124:024904-1-9.

[13] Zong J, Wang Q, J Chem Phys 2013;139:124907-1-12.

[14] Khandpur AK, Forster S, Bates FS, Hamley IW, Ryan AJ, Bras W, Almdal K, Mortensen K,

Macromolecules 1995;28:8796-806.

[15] K. I. Winey, D. A. Gobran, Z. Xu, L. J. Fetters and E. L. Thomas, Macromolecules 27, 2392 (1994).

[16] Ryan AJ, Mai SM, Fairclough JP, Hamley IW, Booth C, Phys Chem Chem Phys 2001;3:2961-2971.

[17] Zhao J, Majumdar B, Schulz MF, Bates FS, Almdal K, Mortensen K, Hajduk DAand, Gruner SM, Macromolecules 1996;29:1204-15.

[18] Floudas G, Vazaiou B, Schipper F, Ulrich R, Wiesner U, Iatrou Hand, Hadjichristidis N, Macromolecules 2001;34:2947-57.

[19] Schmidt SC, Hillmyer MA, J Polym Sci Part B: Polym Phys 2002;40:2364-76.

[20] Lee S, Gillard TM, Bates FS, AIChE J 2013;59:3502-13.

[21] Schulz MF, Khandpur AK, Bates FS, Almdal K, Mortensen K, Hajduk DA, Gruner SM, Macromolecules 1996;29:2857-2867.

[22] Hamley IW, Castelletto V, Yang Z, Price C, Booth C, Macromolecules 2001;34:4079-81.

[23] Hajduk DA, Kossuth MB, Hillmyer MA, Bates FS, J Phys Chem B 2001;102:4269-76.

[24] Vavasour JD, Whitmore MD, Macromolecules 1993;26:7070-5.

[25] Rosedale JH, Bates FS, Almdal K, Mortensen K, Wignall GD, Macromolecules 1995;28:1429-43.

[26] Maurer WM, Bates FS, Lodge TP, Almdal K, Mortensen K, Fredrickson GH, J Chem Phys 1998;108:2989-3000.

[27] Matsen MW, Macromolecules 2012;45:8502-9.

[28] Mori K, Hasegawa H, Hashimoto T, Polymer 2001;42:3009-21.

[29] He XN, Xu JT, Prog Polym Sci 2012;37:1350-1400.

[30] Takagi H, Yamamoto K, Okamoto S, Sakurai S, Polymer 2010;51:4160-8.

[31] Nojima S, Nakano H, Takahashi Y, Ashida T, Polymer 1994;35:3479-86.

[32] Takagi H, Yamamoto K, Okamoto S, Shinichi S, Kobunshi Ronbunshu 2009;66:442-9.

[33] Stuhn B, Mutter R, Albrecht T, Europhys Lett 1992;18:427-32.

[34] Bates FS, Rosedale JH, Fredrickson GH, J Chem Phys 1990;92:6255-70.

[35] Hashimoto T, Ogawa T, Han CD, J Phys Soc Jpn 1994;63:2206-14.

[36] Winey KI, Gobran DA, Xu Z, Fetters LJ, Thomas EL, Macromolecules 1994;27:2392-7.

[37] Almdal K, Mortensen K, Ryan AJ, Bates FS, Macromolecules 1996;29:5940-7.

[38] Wolff T, Burger C, Ruland W, Macromolecules 1993;26:1707-11.

[39] Han CD, Vaidya NY, Yamaguchi D, Hashimoto T, Polymer 2000;41:3779-89.

[40] Herrera D, Zamora JC, Bello A, Grimau M, Laredo E, Muller AJ, Lodge TP, Macromolecules 2005;38:5109-17.

[41] Bates FS, Dierker SB, Wignall GD, Macromolecules 1986;19:1938-45.

[42] Lai C, Russel WB, Register RA, Marchand GR, Adamson DH, Macromolecules 2000;33:3461-6.

[43] Sakamoto N, Hashimoto T, Macromolecules 1995;28:6825-34.

[44] Floudas G, Pakula T, Velis G, Sioula S, Hadjichristidis N, J Chem Phys 1998;108:6498-501.

[45] Han CD, Beak DM, Kim JK, Ogawa T, Sakamoto N, Hashimoto T, Macromolecules 1905;28:5043-62.

[46] Zha W, Han CD, Lee DH, Han SH, Kim JK, Kang JH, Park C, Macromolecules 2007;40:2109-19.

[47] Han CH, Lee DH, Kim JK, Macromolecules 2007;40:7416-9.

[48] Zhao Y. Sivaniah E, Hashimoto T, Macromolecules 2008;41:9948-51.

[49] Almdal K, Hillmyer MA, Bates FS, Macromolecules 2002;35:7685-91.

[50] Mansour AS, Johnson LF, Lodge TP, Bates FS, J Polym Sci Part B: Polym Phys 2010;48:566-74.

Table and Figure captions.

Table1. Molecular and morphological characteristics of diblock copolymers

Table 2. T_{ODT}, calculated N and $(\chi N)_{ODT}$ for PCL-PB

Table 3. Summary of the molecular characteristics of various block copolymers

Table 4. Summary of interaction parameter reported in the literature for various block copolymers

FIG. 1. Temperature dependence of SAXS profiles for BCL9 in heating process.

FIG. 2. I_m^{-1} (Inverse of the scattered intensity at q*) and σ_q^2 (square of full-width at half-maximun at q*) plotted as a function of 1/T for BCL9, where q* is the q-value at the first-order scattering maximum.

FIG. 3. Characteristic length D (=2π/q*) plotted as a function of 1/T.

FIG. 4. Best fits between experimental and theoretical scattering profiles for BCL9 at 120, 140, 160, 180 and 200 °C. The solid curves are calculated scattering profiles using eq. (6).

FIG. 5. The temperature dependence of χ obtained from eq. (6) for BCL9.

FIG. 6. Experimentally obtained PCL-PB phase diagram. Solid circles indicate the order-disorder transition determined by SAXS. Open square indicates order-order transition. The solid line is drawn to indicate the different boundary. Thick vertical lines show the range of χN explored by SAXS for each samples. The dashed line is a spinodal line predicted by using eq. (6). Phase notation is as follows: LAM, lamellae; Gyr, gyroid; HEX, hexagonally packed cylinders; BCC, spheres arranged in body centered

cubic lattice.

FIG. 7. The plots of $(cN)_{ODT}$ / $(cN)_{ODT,s}$ -1 versus $\tilde{N}$. The solid line represents theoretical curve predicted by using eq. (1). Detailed data is listed in Table 3. The numbers in brackets correspond to reference number.